# The p53-dependent effects of macrophage migration inhibitory factor revealed by gene targeting

G. Fingerle-Rowson*†‡§, O. Petrenko‡¶, C. N. Metz‖, T. G. Forsthuber**, R. Mitchell*††, R. Huss‡‡, U. Moll¶, W. Müller§§, and R. Bucala¶¶

*The Picower Institute for Medical Research, Manhasset, NY 11030; ¶Department of Pathology, Stony Brook University, Stony Brook, NY 11794; ‖North Shore–Long Island Jewish Research Institute, Manhasset, NY 11030; **Institute of Pathology, Case Western Reserve University, Cleveland, OH 44106; ‡‡Department of Pathology, Ludwig Maximilians University, D-81366 Munich, Germany; §§Department of Experimental Immunology, Gesellschaft für Biotechnologische Forschung, 38124 Braunschweig, Germany; and ¶¶Department of Medicine and Pathology, Yale University School of Medicine, New Haven, CT 06520

Communicated by George J. Todaro, Targeted Growth, Inc., Seattle, WA, May 30, 2003 (received for review January 9, 2003)

**Macrophage migration inhibitory factor (MIF) is a mediator of host immunity and functions as a high, upstream activator of cells within the innate and the adaptive immunological systems. Recent studies have suggested a potentially broader role for MIF in growth regulation because of its ability to antagonize p53-mediated gene activation and apoptosis. To better understand MIF's activity in growth control, we generated and characterized a strain of MIF-knockout (MIF-KO) mice in the inbred, C57BL/6 background. Embryonic fibroblasts from MIF-KO mice exhibit p53-dependent growth alterations, increased p53 transcriptional activity, and resistance to *ras*-mediated transformation. Concurrent deletion of the p53 gene *in vivo* reversed the observed phenotype of cells deficient in MIF. *In vivo* studies showed that fibrosarcomas induced by the carcinogen benzo[$\alpha$]pyrene are smaller in size and have a lower mitotic index in MIF-KO mice relative to their WT counterparts. The data provide direct genetic evidence for a functional link between MIF and the p53 tumor suppressor and indicate an important and previously unappreciated role for MIF in carcinogenesis.**

carcinogenesis | cytokines | p21 | transformation

Macrophage migration inhibitory factor (MIF) is considered to be the first "cytokine" discovered, and it was identified initially for its ability to inhibit the random migration of macrophages in culture (1). MIF was described originally to be a product of activated T cells, but the protein is now known to be produced by a variety of mesenchymal, parenchymal, and epithelial cell types (reviewed in ref. 2). The primary focus of MIF research has been in the context of its role in immunological function, and studies that used pure recombinant MIF and MIF-specific antibodies have established a role of MIF in the pathogenesis of septic shock (3), inflammatory arthritis (4), glomerulonephritis (5), allograft rejection (6), and wound repair (7). At the cellular level, MIF has been reported to antagonize the action of glucocorticoids and to promote the production of proinflammatory mediators (reviewed in ref. 2). The molecular mechanism of MIF action remains incompletely defined, but there is evidence that MIF induces both known and still uncharacterized signal transduction pathways.

Recent studies (8, 9) have implicated MIF as a regulator of cell growth and apoptosis. MIF expression patterns change during organogenesis and tissue specification and they are influenced by growth inhibition *in vivo* (10). High levels of MIF expression have been observed in several human cancers and expression correlates with tumor grading and clinical prognosis (11–15). Kleemann *et al.* (16) have provided evidence for an intracellular function of MIF in the regulation of cell growth through binding to Jab1, a subunit of the COP9 signalosome complex, which has been implicated in signaling pathways and protein degradation (17, 18). Using cell-based genetic screens, Hudson *et al.* (19) have demonstrated that MIF interacts with the p53 tumor suppressor by inhibiting p53-responsive gene activation and apoptosis. The high frequencies of mutations in the p53 gene that are found in human tumors (20), and the apparent correlation of p53 loss with tumor aggressiveness (21) emphasize the importance of p53 as a "gatekeeper" in the development of neoplastic disease. Accordingly, it has been hypothesized that the bypass of p53 regulatory functions by MIF at sites of chronic inflammation might impair the normal response to genetic damage, enhance cell proliferation, and promote the accumulation of oncogenic mutations (22).

To better understand the association of MIF with growth control and neoplastic disease, we have generated MIF-knockout (MIF-KO) mice on the pure C57BL/6 background. The results described herein provide direct support for a functional link between MIF and p53, and implicate MIF as a novel regulator of carcinogenesis.

## Materials and Methods

**Generation of MIF-Deficient Mice.** A genomic DNA fragment containing the *MIF* gene was isolated from a 129/Sv P1 library (Incyte Genomics, Palo Alto, CA). A 5.2-kb *Pst*I–*Bgl*II fragment containing the *MIF* gene, including the promoter region and exons 1, 2, and 3, was cloned between the *loxP* sites of the vector pEasyFlox (kindly provided by M. Alimzhanov, Institute of Genetics, Cologne, Germany). Additional regions of homology (a 6-kb upstream and a 3.8-kb downstream fragment) flanking the *MIF* locus were cloned into pEasyFlox before and after the *loxP* sites, respectively (Fig. 1). C57BL/6 embryonic stem (ES) cells were transfected with the targeting vector and subjected to double selection with G418 and gancyclovir. Targeted ES cell clones were identified by Southern blot hybridization using external 5′ and 3′ probes. Two targeted ES clones were transiently transfected with a plasmid expressing Cre recombinase. ES clones deleted for both *MIF* and *neo* were microinjected into BALB/c blastocysts. Chimeras gave germ-line transmission and the offspring were bred to homozygosity to produce a population of MIF-KO mice on the pure C57BL/6 background.

$MIF^{-/-}p53^{-/-}$ double-KO (DKO) mice were generated by crossing between the MIF-KO and previously reported $Trp53^{tm1Tyj}$ mice (23). The genotype of each group of mice was verified by PCR amplification specific for the corresponding WT and mutant alleles. Primer sequences are available on request.

**Cells and Tissue Culture.** Mouse embryonic fibroblasts (MEFs) were prepared from embryonic day 14.5 embryos from the $MIF^{+/+}$, $MIF^{-/-}$, $p53^{-/-}$, and $MIF^{-/-}p53^{-/-}$ mice using standard tech-

Abbreviations: MIF, macrophage migration inhibitory factor; MIF-KO, MIF-knockout; DKO, double KO; ES, embryonic stem; MEF, mouse embryonic fibroblast; Rb, retinoblastoma; ERK, extracellular-regulated kinase.

†Present address: GSF/Haematologikum, Klinische Kooperationsgruppe Gentherapie, Marchioninistrasse 25, 81377 Munich, Germany.

‡G.F.-R. and O.P. contributed equally to this work.

§To whom correspondence should be addressed at: GSF/Haematologikum, KKG Gentherapie, Labor 042, Marchioninistrasse 25, D-81377 Munich, Germany. E-mail: g.fingerle-rowson@gmx.de.

††Present address: J. G. Brown Cancer Center, University of Louisville, Louisville, KY 40202.

 www.pnas.org/cgi/doi/10.1073/pnas.1533295100

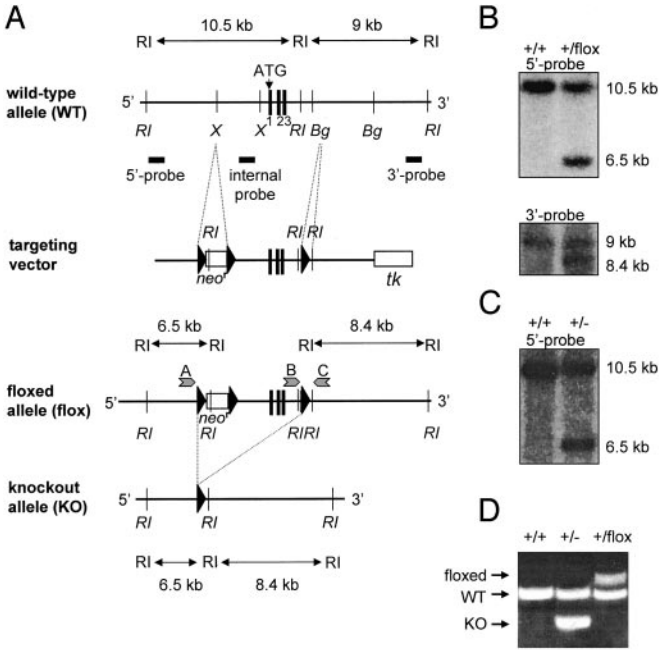


**Fig. 1.** Generation of *MIF* mutant mice. (*A*) A schematic representation of the *MIF*-WT allele (exons 1, 2, and 3, *Top*), the targeting vector, the allele flanked by loxP sites (floxed allele), and the KO allele (*Bottom*). Bg, *Bgl*II; RI, *Eco*RI; X, *Xba*I; tk, thymidine kinase; ATG, translation initiation codon. In targeted ES cells, the *MIF* gene and the neomycin-resistance cassette (*neo*$^r$), both flanked by the *loxP* sites, were subsequently deleted by Cre-mediated recombination. (*B*) Southern blot analysis of WT and floxed (*neo*$^r$) alleles using *Eco*RI-digested genomic DNA and external hybridization probes. (*C*) G418-sensitive ES clones, derived after *neo*$^r$ deletion, were analyzed by Southern hybridization using *Eco*RI-digested genomic DNA and the 5′ probe. (*D*) PCR amplification using ES-derived genomic DNA and primers specific for the WT (544 bp), floxed (683 bp), and MIF-KO (383 bp) alleles. The position of the primers A, B, and C is indicated in *A* for the floxed allele.

niques. In some experiments, as indicated, we used MEFs that were derived from reported MIF-KO mice (24) that were backcrossed to the BALB/c background for six generations. Unless specified, passage 4–6 MEFs were used.

**Retroviral Constructs.** The replication-defective retroviral vector REBNA (25) was used. For viral infections, $10^5$ MEFs cultured in 6-cm plates were incubated overnight with an appropriate amount of the corresponding retroviral stock.

**Expression Analyses.** The list of antibodies is available on request.

**One-Stage Carcinogenesis Model.** C57BL/6 female, 12- to 16-week-old WT and MIF-KO littermates ($n = 20$ per group) were injected s.c. in the right flank with 2 mg of benzo[$\alpha$]pyrene (Sigma) in 200 $\mu$l of olive oil on days 1 and 8. Mice were killed when tumor incidence reached 100% in the WT group (week 16) and tumors were processed for pathological examination. Tumor vascularization was assessed by immunohistochemical staining for smooth muscle actin (HHF35; DAKO).

**Two-Stage Carcinogenesis Model.** Eight- to 12-week-old, BALB/c WT and MIF-KO females (gift of J. David, Harvard Medical School, Boston; $n = 15$ per group) were shaved and 25 $\mu$g of 7,12-dimethylbenz[$\alpha$]anthracene (DMBA) in 100 $\mu$l of acetone was applied to intact skin on days 1 and 8. Tumor formation was promoted by using 12-*O*-tetradecanoylphorbol 13-acetate (TPA; 4 $\mu$g in 100 $\mu$l acetone, three times a week) for 23 weeks.

**Statistical Analysis.** Data are expressed as mean ± SD. Statistical analysis was performed by using a two-tailed Student's *t* test.

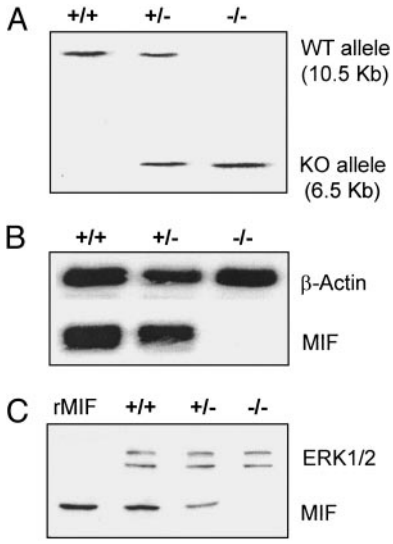


**Fig. 2.** Validation of the MIF-KO mouse. (*A*) *Eco*RI-digested genomic DNA prepared from WT (+/+), heterozygous (+/−), and MIF-KO (−/−) mice was hybridized with the external 5′ probe. (*B*) Northern blot analysis of RNA prepared from the spleens of WT (+/+), heterozygous (+/−), and MIF-KO mice (−/−) using *MIF* cDNA as probe. (*C*) Immunoblot analysis of protein extracts prepared from the livers of WT (+/+), heterozygous (+/−), and MIF-KO mice (−/−) using a MIF-specific polyclonal antibody (R102). The expression of mitogen-activated protein kinase ERK1/2 is shown as a loading control. rMIF, recombinant MIF.

## Results

**Generation of MIF-KO Mice.** MIF-KO mice have been recently reported by two research groups (24, 29). These two mouse strains show an inconsistency in their immunological phenotype (resistance to endotoxic shock), which may be due to the mixed genetic background in which they were created, or to the gene targeting strategies. To obviate these difficulties, we elected to use the Cre-loxP gene targeting technique (26) and C57BL/6 ES cells to generate a complete (5.2 kb) deletion of the *MIF* locus in a pure genetic background. The deletion included (from 5′ to 3′): the 3′ end of a nonfunctional retrotransposon of the intracisternal A-particle type (IAP) located upstream of the *MIF* gene (27), the promoter of the *MIF* gene, and *MIF* exons 1, 2, and 3 (Fig. 1*A*). Homologous recombination of the targeting vector was confirmed by Southern hybridization by using 5′ and 3′ external probes (Fig. 1*B*). Because *neo*-containing selectable cassettes have the potential to affect the expression of genes over distances of >100 kb (28), we chose to excise the *loxP*-flanked neomycin-resistance marker by using a transiently expressed Cre recombinase. Correct excision of the MIF gene was verified by Southern blotting (Fig. 1*C*), and by PCR specific for the WT and the MIF-KO alleles (Fig. 1*D*).

After blastocyst injection and germ-line transmission of the chimeric mice, MIF$^{+/-}$ heterozygous mice were bred in the genetically pure, C57BL/6 background. Southern analysis of genomic DNA and Northern hybridization of cellular RNA derived from the tissues of WT, heterozygous MIF$^{+/-}$, and homozygous MIF$^{-/-}$ KO mice confirmed the deletion of the *MIF* gene (Fig. 2 *A* and *B*). Consistent with this finding, immunoblot analysis (R102) showed no MIF expression in the MIF-KO mice (Fig. 2*C*).

Mice with the MIF-KO genotype are born at the expected Mendelian ratios in the heterozygous intercrosses (MIF$^{+/+}$: MIF$^{+/-}$: MIF$^{-/-}$ in males 39:69:35; in females 36:93:47). MIF-KO mice show no developmental abnormalities, are fertile, and produce litters of normal size (6.5 pups per litter, $n = 32$ litters). The spontaneous death rate of MIF-KO mice is low and similar to that of WT littermates. At 6 weeks of age, the weight of MIF-KO mice also was comparable to that of control WT mice (males: MIF$^{+/+}$

CELL BIOLOGY

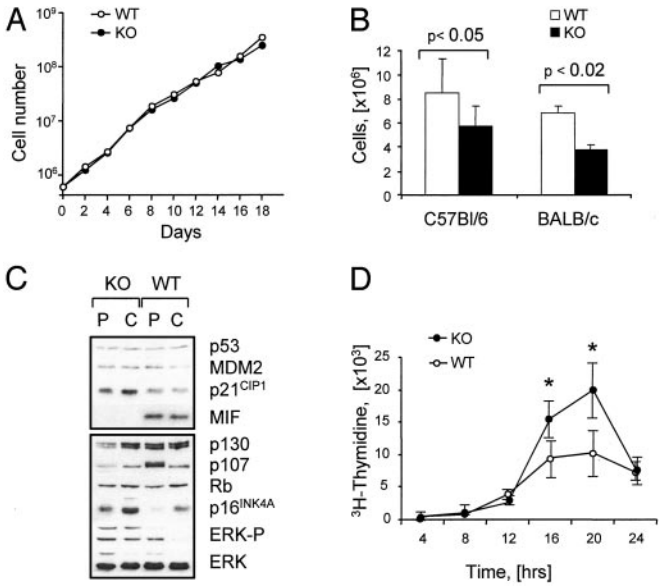


**Fig. 3.** The growth properties of primary MIF-KO fibroblasts. (*A*) Representative growth curves of MIF-KO and WT embryonic fibroblasts. (*B*) MIF-KO and WT fibroblasts were grown in 10-cm plates, and the cell density of cultures was determined 4 days after visible confluency. The data were derived from four independent experiments. (*C*) Immunoblot analysis of proliferating (P) and confluent (C) MIF-KO and WT fibroblasts. (*D*) MIF-KO and WT fibroblasts were synchronized in G0G1 by serum starvation and were then induced by serum to re-enter the cell cycle. The proportion of cells in S phase was determined by $^3$H-thymidine incorporation. *, $P < 0.01$.

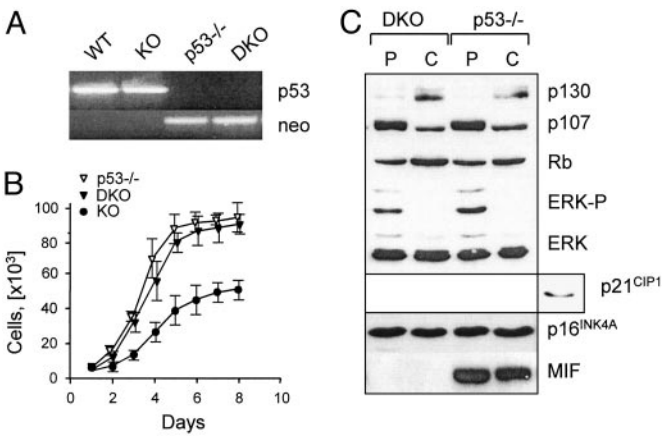


**Fig. 4.** Growth characterization of MIF$^{-/-}$p53$^{-/-}$ DKO fibroblasts. (*A*) The deletion of the *Trp53* gene in DKO mice was confirmed by PCR amplification, using the primers specific for the p53 WT and KO (neo) allele. (*B*) Representative growth curves of p53$^{-/-}$, DKO, and MIF-KO fibroblasts. (*C*) Immunoblot analysis of proliferating (P) and confluent (C) DKO and p53$^{-/-}$ fibroblasts with the indicated antibodies. The expression of p21 by MIF-KO MEFs (*Right*) is shown as a control.

18.2 ± 1.7 g, MIF$^{-/-}$ 18.8 ± 2.4 g; females: MIF$^{+/+}$ 16.2 ± 1.1 g, MIF$^{-/-}$ 16.4 ± 1.3 g, $P$ = not significant, $n = 16$ per group). Flow cytometric analysis of leukocyte subsets from the peripheral blood of MIF-KO mice showed no abnormalities in the distribution of lymphoid or myeloid lineages compared with WT mice (data not shown).

**Growth Alterations in MIF-KO Fibroblasts.** Previous studies (19) suggested that MIF may act as a functional p53 antagonist. To examine this possibility, MEFs were prepared from MIF-KO and WT mice and characterized in cell-based assays. Exponentially growing MIF-KO and WT fibroblasts showed similar proliferation rates (Fig. 3*A*). However, MIF-KO fibroblasts growth arrested at saturating cell densities that were 20–30% lower compared with that of WT MEFs (Fig. 3*B*). Similar results were obtained by using WT and MIF-KO fibroblasts derived from the respective BALB/c mice (Fig. 3*B*).

Immunoblot analyses of continuously cycling WT and MIF-KO fibroblasts showed similar expression levels for p53 and its downstream target products, such as p21$^{CIP1}$ (p21) and MDM2 (Fig. 3*C*). However, cycling MIF-KO fibroblasts showed increased levels of the activated (phospho) extracellular-regulated kinase (ERK)-1/2. By contrast, the expression levels of the retinoblastoma protein (Rb)-related cell-cycle regulators, p107 and p130, were lower in cycling MIF-KO fibroblasts (Fig. 3*C*). It has been shown that Rb, p107, and p130 regulate the activity of E2F transcription factors in a cell type-specific manner at different stages of the cell cycle (30). Whereas p130 appears to be prominent in quiescent and differentiated cells (31, 32), p107 is the most abundant Rb-related protein present in the nuclei of S-phase cells (33, 34). Consistent with these observations, synchronized MIF-KO fibroblasts entered the S-phase and completed DNA synthesis in a uniform fashion, as assessed by $^3$H-thymidine incorporation (Fig. 3*D*). Although p107 is a direct target for E2F-regulation (35), the expression of several other E2F-responsive gene products, including cyclin A, cyclin E, CDC6, and B-Myb, was similar in both the MIF-KO and the WT cells (data not shown). Collectively, these results suggest that the growth alteration observed in MIF-KO fibroblasts is likely due to the induction of premature arrest, rather than to a defect in cell division.

**Premature Growth Arrest in MIF-KO Fibroblasts Is p53-Dependent.** The growth arrest in MIF-KO MEFs was associated with higher expression levels of p16$^{INK4A}$ (p16), and the downstream target of p53, p21$^{CIP1}$ (Fig. 3*C*). It has been noted that mitogen-activated protein kinase (MAPK) activation involves up-regulation of p53 and p16 (36). Conversely, continuous expression of p53 results in a sustained activation of the MAPK cascade by a mechanism involving the epidermal growth factor receptor (37, 38). To determine whether the growth differences between the MIF-KO and WT fibroblasts could be attributed to the altered status of p53 in MIF-KO cells, we produced MIF$^{-/-}$p53$^{-/-}$ DKO mice by crossing the MIF-KO mice with p53$^{-/-}$ mice, both on the C57BL/6 background (23). The deletion of both the *MIF* and the *Trp53* genes was confirmed by PCR and Western blot analyses (Fig. 4 *A* and *C*). MEFs derived from DKO and p53$^{-/-}$ mice exhibited similar proliferation properties (Fig. 4*B*). Closer examination showed equivalent expression levels of p130, p107, and p16 by DKO and p53$^{-/-}$ MEFs, whereas p21 was not expressed at detectable levels (Fig. 4*C*). The levels of ERK phosphorylation also were similar between the two cell types (Fig. 4*C*). Taken together, these results indicate that the growth alterations observed in MIF-KO fibroblast are to a large degree p53-dependent.

**MIF Modulates DNA Damage-Induced p53 Transactivation.** Various stress conditions, including DNA damage, oncogene activation, and hypoxia can induce a p53-specific response (39). We next assessed p21 activation in MIF-KO and WT MEFs after exposure to the DNA-damaging agent, cisplatin. The induction of p21 expression was more pronounced in the MIF-KO than in the WT fibroblasts (Fig. 5 *A* and *B*). This induction of p21 also was p53-dependent, because DKO MEFs failed to accumulate detectable p21 protein when exposed to similar stress conditions (Fig. 5*C*).

**The Reduced Susceptibility of MIF-KO Fibroblasts to Ras-Mediated Transformation Is p53-Dependent.** The incorporation of activated oncogenes into rodent cells induces p53-dependent replicative

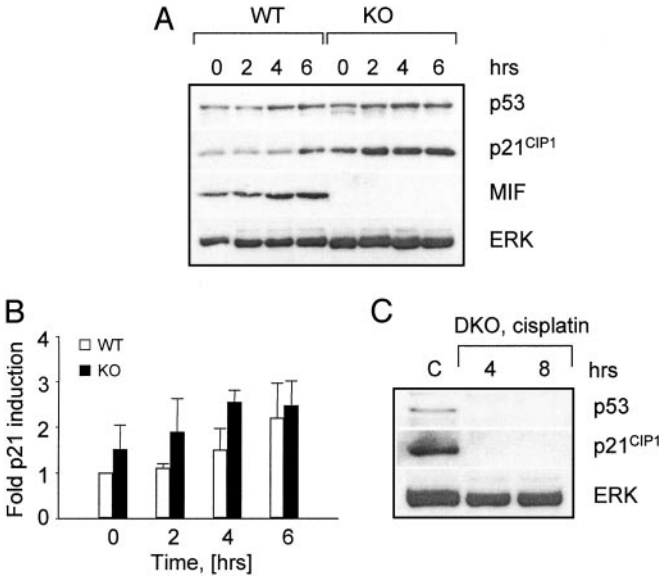


**Fig. 5.** MIF modulates cisplatin-induced p53 transactivation. (*A*) Immunoblot analysis of p53, p21, and MIF expression by MIF-KO and WT MEFs incubated in the presence of 25 $\mu$M cisplatin. (*B*) Relative expression of p21 by MIF-KO and WT MEFs at the indicated periods of time after cisplatin treatment. Densitometric measurements were converted into fold induction relative to untreated WT MEFs. (*C*) Immunoblot analysis of DKO fibroblasts exposed to 25 $\mu$M cisplatin (cp) for 4 and 8 h. Untreated MIF-KO fibroblasts (C) are shown as controls.

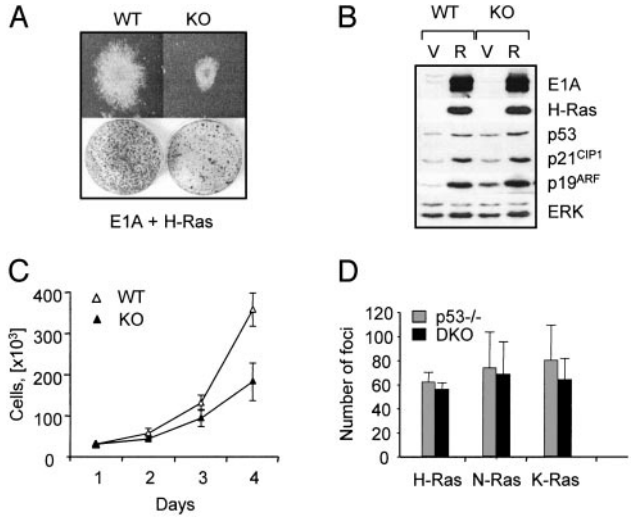


**Fig. 7.** The reduced susceptibility of MIF-KO fibroblasts to *ras*-mediated transformation is p53-dependent (*A*) Focus formation by MIF-KO and WT fibroblasts coexpressing E1A and H-*ras*$^{V12}$. (*Upper*) Representative morphology of a single colony induced by E1A and H-*ras*$^{V12}$ in MIF-KO and WT MEFs ($\times$10 magnification). (*B*) Western blot analysis of MIF-KO and WT MEFs infected with empty vector (V)- or E1A- and H-*ras*$^{V12}$ (R)-containing retroviruses. (*C*) Growth curves of MIF-KO and WT fibroblasts coexpressing E1A and H-*ras*$^{V12}$. (*D*) Focus formation by p53$^{-/-}$ and MIF$^{-/-}$p53$^{-/-}$ DKO fibroblasts expressing H-Ras$^{V12}$, N-Ras$^{D12}$, or K-Ras$^{V12}$ mutants.

arrest and the expression of senescence-associated markers (40). Transduction of MIF-KO and WT fibroblasts with replication-defective retroviruses expressing a constitutively active H-*ras*$^{V12}$ mutant also produced growth inhibition (Fig. 6*A*). The expression of the negative cell-cycle regulators, p53, p19$^{ARF}$ (ARF), Rb, and p16, was similar between the two cell types (data not shown). However, the induction of senescence-like morphology and the expression of senescence-associated $\beta$-galactosidase (SA-$\beta$ Gal), were more rapid in the H-*ras*$^{V12}$-transduced MIF-KO cells than in the corresponding WT transductants (Fig. 6*B*).

Tumor cell growth is frequently associated with a disruption of the Rb tumor suppressor pathway (41). We next expressed H-*ras*$^{V12}$ in conjunction with the adenovirus E1A protein. E1A-expressing fibroblasts behave like Rb-deficient cells in that their increased proliferative capacity is accompanied by an increased sensitivity to E2F1- and p53-dependent apoptosis (42). In several independent experiments, MIF-KO MEFs coexpressing E1A and *ras* produced transformed colonies with a 50% lower efficiency when compared with the corresponding WT MEFs, as assessed by focus formation assays (Fig. 7*A* and Table 1). Immunoblot analysis of the transformed MIF-WT and KO cells showed similar levels of E1A expression (Fig. 7*B*). The levels of E1A binding to the Rb family proteins also were similar in the two cell types (data not shown). However, the differences in colony formation between MIF-KO and WT MEFs correlated with a generally lower proliferation rate by the transformed MIF-KO cultures (Fig. 7*C*), and by smaller transformed foci (Fig. 7*A Upper*). Similar results were obtained by using *myc*- and *ras*-transformed MIF-WT and KO fibroblasts (Table 1).

To test whether the differences in the transforming capacity of MIF-KO fibroblasts were p53-dependent, we studied the effect of the simian virus 40 large T-antigen (LT), the oncogenic properties of which depend on its ability to inactivate both Rb and p53 (43). After the introduction of oncogenic *ras*, LT-expressing MIF-KO and WT fibroblasts were readily transformed and produced equally numerous foci and soft agar colonies (Table 1). Similarly, expression of constitutively active H-*ras*$^{V12}$, N-*ras*$^{D12}$, or K-*ras*$^{V12}$ mutants in p53$^{-/-}$ and DKO fibroblasts resulted in equivalent transformation efficiency (Fig. 7*D*). These results are consistent with the reported ability of MIF to modulate p53 activity (19). This MIF

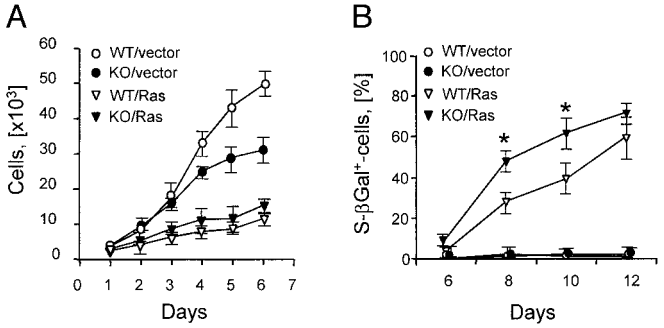


**Fig. 6.** Induction of *ras*-mediated senescence response in MIF-deficient fibroblasts. (*A*) Growth curves of MIF-KO and WT fibroblasts after infection with empty vector (V)- or H-*ras*$^{V12}$ (R)-expressing retroviruses. (*B*) Kinetics of SA-$\beta$Gal expression by MIF-KO and WT fibroblasts infected with V- or R-expressing retroviruses. *, $P < 0.02$.

**Table 1. The transforming properties of WT and MIF-KO fibroblasts**

| MEF type | Oncogene combination | Transformed foci per plate | No. of experiments | Significance, *P* |
|---|---|---|---|---|
| WT | E1A, H-Ras | 688 ± 128 | 8 | 0.00002 |
| KO | E1A, H-Ras | 332 ± 42 | 8 | |
| WT | c-Myc, H-Ras | 44 ± 13 | 8 | 0.0002 |
| KO | c-Myc, H-Ras | 18 ± 10 | 8 | |
| WT | LT, H-Ras | 166 ± 32 | 6 | 0.5 |
| KO | LT, H-Ras | 168 ± 29 | 6 | |

Each experiment was performed in triplicate with separate WT and MIF-KO MEF batches. Equivalent expression levels of the corresponding oncogenes were confirmed by Western blot analyses.

CELL BIOLOGY

effect does not involve down-regulation of ARF expression, because the transformed MIF-KO and WT fibroblasts contained equivalent levels of the ARF protein (Fig. 7*B*).

**Reduced Development of Benzo[α]pyrene-Induced Fibrosarcomas in MIF-Deficient Mice.** To directly address the possibility that MIF plays a role in the generation of the transformed phenotype, we studied tumorigenesis in MIF-KO mice. Initially, we used a two-stage protocol of skin carcinogenesis, which includes the application of DMBA, followed by multiple applications of TPA. This approach results in the development of benign skin tumors that often contain a characteristic mutation in the codon 61 of the cellular H-*ras* gene but retain intact p53 (44). Because C57BL/6 mice are relatively resistant to skin carcinogenesis (45), we used MIF-KO mice (24), which were backcrossed to the BALB/c background for six generations. During the time course of this experiment, tumor incidence and multiplicity were similar between the MIF-KO and WT mice (Fig. 8*A*). Because *ras*-mediated tumorigenesis depends on signaling pathways that act through cyclin D1 (46), our results indicate that the Ras-MAPK-cyclin D1 pathway is fully functional in MIF-KO cells *in vivo*. Tumor regression began earlier in MIF-KO mice than in the WTs ($P < 0.05$).

In a second approach, 12- to 16-week-old female C57BL/6 MIF-KO and WT mice were injected s.c. in the right flank with the carcinogen, benzo[α]pyrene (B[α]P). Treatment with B[α]P produces stochastic mutations, which frequently involve cellular protooncogenes such as *ras*, and tumor suppressor genes, including *Trp53* (47, 48). Mutations that concurrently occur within the context of a single cell then will result in tumorigenic conversion. Within 4 months, all of the MIF-KO and WT mice injected with B[α]P developed sizable tumors. Histologically, tumors from both genotypes were characterized as high-grade fibroleiomyosarcomas (smooth muscle actin-positive, mitotic index >20/10 high power fields). Although no differences were found between the MIF-WT and KO mice with respect to tumor incidence, MIF deficiency was associated with a lower mitotic rate ($MIF^{+/+}$ 79 ± 26, $MIF^{-/-}$ 46 ± 10 mitoses/10 high-power fields, Fig. 8 *B* and *C Upper*, $P = 0.003$) and smaller tumor size ($MIF^{+/+}$ 2.6 ± 1.7 g, $MIF^{-/-}$ 1.3 ± 0.9 g, $P = 0.002$). Tumor tissues from MIF-KO and MIF-WT smooth muscle actin (SMA)-positive vessels and SMA-negative small capillaries were vascularized similarly. Areas of necrosis were present in tumors from both genotypes, but were larger in the MIF-WT hosts (Fig. 8*C Lower*), which may be a result of hypoxia or acidosis developing in faster growing tumors.

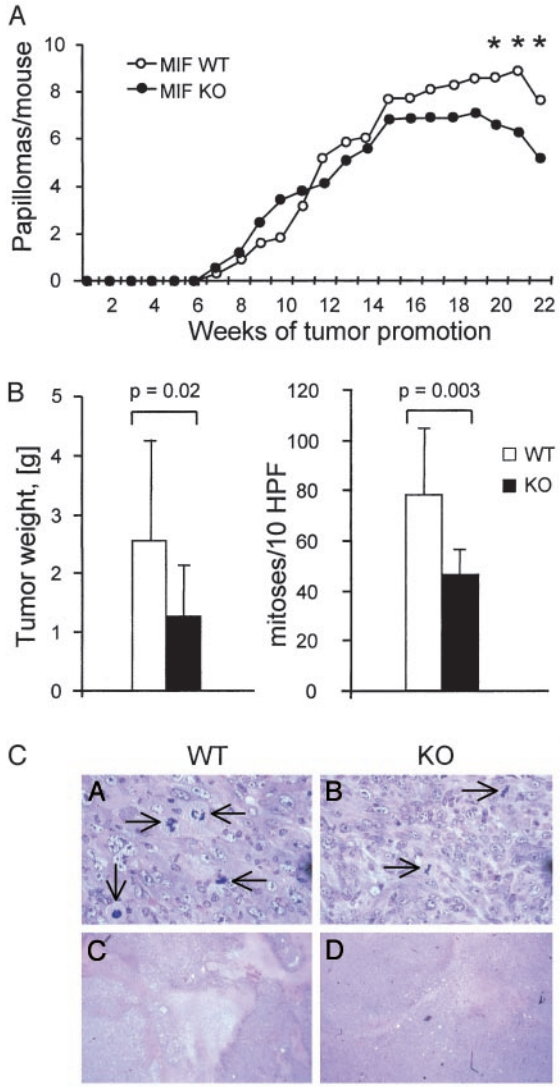


**Fig. 8.** MIF-deficient mice exhibit delayed development of B[α]P-induced fibrosarcomas. (*A*) Tumor development by MIF-KO and WT BALB/c mice after treatment with DMBA as a tumor initiator and TPA as a promoter. *, significant with $P < 0.05$. (*B*) Tumor formation by C57BL/6 MIF-KO and WT mice after injection of B[α]P. (*Left*) Tumors developed by MIF-KO, and WT mice were excised in week 16 and weighed ($P = 0.02$). (*Right*) Mitotic index in B[α]P-induced fibrosarcomas from MIF-KO and WT mice ($P = 0.003$). (*C*) Histological examination of B[α]P-induced tumors in C57BL/6 MIF-KO and WT mice. Hematoxylin/eosin stain. Magnification: *Upper*, ×400; *Lower*, ×5. Arrowheads indicate cells undergoing mitoses.

## Discussion

Macrophage MIF is an important regulator of host immunity as evidenced by numerous experimental and clinical studies (2). Another spectrum of action for MIF has emerged as the result of the finding by Hudson *et al.* (19) that MIF inhibits p53-transcriptional activity in cell-based, functional assays. MIF overexpression was found to extend the lifespan of fibroblasts *in vitro*, to inhibit *myc*-induced p53-dependent apoptosis, and to protect macrophages from NO-induced apoptosis. The potential importance of this activity has increased in the light of studies showing that MIF is expressed in different human tumors, and at levels that may correlate with tumor aggressiveness (11–15, 49).

To test the relevance of MIF as a growth regulator, we generated a strain of MIF-KO mice on the pure C57BL/6 background. Consistent with previous reports (24, 29), MIF deficiency did not cause any obvious developmental defects. The MIF-KO mice nevertheless exhibit a distinct phenotype with respect to growth control and tumorigenesis. Cultured embryonic fibroblasts derived from these mice showed increased sensitivity to contact inhibition and resistance to *ras*-mediated transformation. Importantly, both of these properties are largely p53-dependent and appear to result from enhanced p53 transcriptional activity in the MIF-KO cells. These observations were validated *in vivo* by studies showing retardation in the development of malignant tumors in MIF-KO mice when compared with WT controls.

A previous study (50) has shown that MIF can influence cell growth and transformation *in vitro* in cells on the mixed 129/Sv × C57BL/6 background, however the mechanisms were suggested to reflect both p53-dependent and p53-independent pathways. Whereas the p53-independent effects of MIF deficiency rely primarily on the inappropriate induction of E2F transcriptional activity, this article clearly indicates that the E2F-dependent phenotype caused by the loss of MIF is minimal on the pure C57BL/6 background. Moreover, deletion of the p53 gene completely abrogates the effects of MIF deficiency in cells derived from C57BL/6 mice. Differences in the functional status of individual E2F family members between the 129/Sv and C57BL/6 mice have been noted. The loss of *E2f1* extends the lifespan of $Rb^{+/-}$ 129/Sv mice to a

greater extent than in the corresponding C57BL/6 background (51). Conversely, the homozygous deletion of the *E2f3* gene is lethal on the 129/Sv background, whereas the presence of C57BL/6 alleles rescues this phenotype (52). Accordingly, the possibility exists that *MIF*, or a *MIF*-associated gene, acts as a genetic modifier between the 129/Sv and C57BL/6 murine strains.

The p53 tumor suppressor plays at least two distinct roles in preventing inappropriate proliferation: induction of cell-cycle arrest, and induction of apoptosis, which eliminates cells with damaged genomes. Cell-cycle arrest and apoptosis are mechanistically distinct (53), and a spectrum of genes that are controlled by p53 in a positive or negative manner have been identified (54). It is well documented that p53 affects the expression of different groups of genes, depending on the nature of stimuli; however, little is known about the molecular mechanism of p53 action. Several studies have provided information that p53 may change histone acetylation and chromatin condensation at specific chromosomal sites. For example, p53-mediated activation of the p21 gene requires recruitment of histone acetyltransferase (HAT) p300 to the p21 promoter (55), p53-dependent expression of MDM2 involves recruitment of HAT complexes containing the ATM-related TRRAP cofactor (56), and p53-mediated repression of Map4 and stathmin genes relies on an association with histone deacetylase complexes (57). MIF may affect the interaction between p53 and its cofactors.

MIF is remarkably well conserved and its homologues are encoded in evolutionarily divergent species, including different vertebrates, worms [*Caenorhabditis elegans,* (58)], insects [*Amblyomma americanum* (59)], plants [*Arabidopsis thaliana (*60)], and even archaic unicellular eukaryotes, such as *Entamoeba histolytica* (GenBank accession no. AZ542000) and *Giardia intestinalis* (GenBank accession no. AC056441). In *C. elegans*, the role for MIF in growth regulation is supported further by its nuclear localization in developing embryos and by its up-regulation during the dauer stage, a condition of starvation and developmental arrest that allows the nematode to survive adverse conditions (58). In mammals, MIF has been primarily implicated in the pathogenesis of inflammatory disease, based on its increased expression at sites of inflammation and the protective effect of MIF immunoneutralization (2). The role of p53-dependent apoptosis in the immune system is known to be significant during B- and T-lymphopoiesis (61, 62), in protection from genotoxic stressors (63, 64), and in sustaining monocyte/macrophage activation responses (65). This article emphasizes the possibility that inhibition of p53 by MIF may be critical for the development of tumors that arise at sites of chronic inflammation, such as colon cancer in ulcerative colitis (66) and gastric cancer in *Helicobacter pylori* infection (67).

We thank Klaus Rajewsky (Deutsche Forschungsgemeinschaft, SFB 243) and his group from the Institute of Genetics (Cologne, Germany) for their support and advice in gene targeting, and Arlene Sharpe from Harvard Medical School for expert help with blastocyst injections. This work was supported by National Institutes of Health Grants RO1-ARO49610 and RO1-AI42310 (to R.B.), the Picower Foundation (to C.N.M.), and by funds of the Deutsche Forschungsgemeinschaft (Fin 1/1 to G.F.-R.). T.G.F. was supported by National Institutes of Health Grants AI-41609–01, 1RO1AR45918, and NS-42809 and Harry Weaver Neuroscience Scholarship JF-2092-A-1 from the National Multiple Sclerosis Society.

1. David, J. (1966) *Proc. Natl. Acad. Sci. USA* **56,** 72–77.
2. Metz, C. N. & Bucala, R. (2001) in *Cytokine Reference*, eds. Durum, T., Vilcheck, J. & Nicola, N. A. (Academic, San Diego), Vol. 1, pp. 703–716.
3. Bernhagen, J., Calandra, T., Mitchell, R. A., Martin, S. B., Tracey, K. J., Voelter, W., Manogue, K. R., Cerami, A. & Bucala, R. (1993) *Nature* **365,** 756–759.
4. Mikulowska, A., Metz, C. N., Bucala, R. & Holmdahl, R. (1997) *J. Immunol.* **158,** 5514–5517.
5. Lan, H. Y., Bacher, M., Yang, N., Mu, W., Nikolic-Paterson, D. J., Metz, C., Meinhardt, A., Bucala, R. & Atkins, R. C. (1997) *J. Exp. Med.* **185,** 1455–1465.
6. Hou, G., Valujskikh, A., Bayer, J., Stavitsky, A. B., Metz, C. & Heeger, P. S. (2001) *Transplantation* **72,** 1890–1897.
7. Abe, R., Shimizu, T., Ohkawara, A. & Nishihira, J. (2000) *Biochim. Biophys. Acta* **1500,** 1–9.
8. Kobayashi, S., Satomura, K., Levsky, J. M., Sreenath, T., Wistow, G. J., Semba, I., Shum, L., Slavkin, H. C. & Kulkarni, A. B. (1999) *Mech. Dev.* **84,** 153–156.
9. Wistow, G. J., Shaughnessy, M. P., Lee, D. C., Hodin, J. & Zelenka, P. S. (1993) *Proc. Natl. Acad. Sci. USA* **90,** 1272–1275.
10. Fingerle-Rowson, G., Koch, P., Bikoff, R., Lin, X., Metz, C. N., Dhabhar, F. S., Meinhardt, A. & Bucala, R. (2003) *Am. J. Pathol.* **162,** 47–56.
11. Markert, J. M., Fuller, C. M., Gillespie, G. Y., Bubien, J. K., McLean, L. A., Hong, R. L., Lee, K., Gullans, S. R., Mapstone, T. B. & Benos, D. J. (2001) *Physiol. Genomics* **5,** 21–33.
12. Meyer-Siegler, K. & Hudson, P. B. (1996) *Urology* **48,** 448–452.
13. Meyer-Siegler, K. (2000) *J. Interferon Cytokine Res.* **20,** 769–778.
14. del Vecchio, M. T., Tripodi, S. A., Arcuri, F., Pergola, L., Hako, L., Vatti, R. & Cintorino, M. (2000) *Prostate* **45,** 51–57.
15. Tomiyasu, M., Yoshino, I., Suemitsu, R., Okamoto, T. & Sugimachi, K. (2002) *Clin. Cancer Res.* **8,** 3755–3760.
16. Kleemann, R., Hausser, A., Geiger, G., Mischke, R., Burger-Kentischer, A., Flieger, O., Johannes, F. J., Roger, T., Calandra, T., Kapurniotu, A., *et al.* (2000) *Nature* **408,** 211–216.
17. Naumann, M., Bech-Otschir, D., Huang, X., Ferrell, K. & Dubiel, W. (1999) *J. Biol. Chem.* **274,** 35297–35300.
18. Bech-Otschir, D., Kraft, R., Huang, X., Henklein, P., Kapelari, B., Pollmann, C. & Dubiel, W. (2001) *EMBO J.* **20,** 1630–1639.
19. Hudson, J. D., Shoaibi, M. A., Maestro, R., Carnero, A., Hannon, G. J. & Beach, D. H. (1999) *J. Exp. Med.* **190,** 1375–1382.
20. Vogelstein, B., Lane, D. & Levine, A. J. (2000) *Nature* **408,** 307–310.
21. Levine, A. J. (1997) *Cell* **88,** 323–331.
22. Cordon-Cardo, C. & Prives, C. (1999) *J. Exp. Med.* **190,** 1367–1370.
23. Jacks, T., Remington, L., Williams, B. O., Schmitt, E. M., Halachmi, S., Bronson, R. T. & Weinberg, R. A. (1994) *Curr. Biol.* **4,** 1–7.
24. Bozza, M., Satoskar, A. R., Lin, G., Lu, B., Humbles, A. A., Gerard, C. & David, J. R. (1999) *J. Exp. Med.* **189,** 341–346.
25. Petrenko, O., Beavis, A., Klaine, M., Kittappa, R., Godin, I. & Lemischka, I. R. (1999) *Immunity* **10,** 691–700.
26. Rajewsky, K., Gu, H., Kuhn, R., Betz, U. A., Muller, W., Roes, J. & Schwenk, F. (1996) *J. Clin. Invest.* **98,** 600–603.
27. Kobayashi, S., Yoshida, K., Ohshima, T., Esumi, N., Paralkar, V. M., Wistow, G. J. & Kulkarni, A. B. (1998) *Gene* **215,** 85–92.
28. Pham, C. T., MacIvor, D. M., Hug, B. A., Heusel, J. W. & Ley, T. J. (1996) *Proc. Natl. Acad. Sci. USA* **93,** 13090–13095.
29. Honma, N., Koseki, H., Akasaka, T., Nakayama, T., Taniguchi, M., Serizawa, I., Akahori, H., Osawa, M. & Mikayama, T. (2000) *Immunology* **100,** 84–90.
30. Mulligan, G. & Jacks, T. (1998) *Trends Genet.* **14,** 223–229.
31. Cobrinik, D., Whyte, P., Peeper, D. S., Jacks, T. & Weinberg, R. A. (1993) *Genes Dev.* **7,** 2392–2404.
32. Corbeil, H. B., Whyte, P. & Branton, P. E. (1995) *Oncogene* **11,** 909–920.
33. Schwarz, J. K., Devoto, S. H., Smith, E. J., Chellappan, S. P., Jakoi, L. & Nevins, J. R. (1993) *EMBO J.* **12,** 1013–1020.
34. Moberg, K., Starz, M. A. & Lees, J. A. (1996) *Mol. Cell. Biol.* **16,** 1436–1449.
35. Classon, M., Salama, S., Gorka, C., Mulloy, R., Braun, P. & Harlow, E. (2000) *Proc. Natl. Acad. Sci. USA* **97,** 10820–10825.
36. Lin, A. W., Barradas, M., Stone, J. C., van Aelst, L., Serrano, M. & Lowe, S. W. (1998) *Genes Dev.* **12,** 3008–3019.
37. Lee, S. W., Fang, L., Igarashi, M., Ouchi, T., Lu, K. P. & Aaronson, S. A. (2000) *Proc. Natl. Acad. Sci. USA* **97,** 8302–8305.
38. Fang, L., Li, G., Liu, G., Lee, S. W. & Aaronson, S. A. (2001) *EMBO J.* **20,** 1931–1939.
39. Prives, C. & Hall, P. A. (1999) *J. Pathol.* **187,** 112–126.
40. Serrano, M., Lin, A. W., McCurrach, M. E., Beach, D. & Lowe, S. W. (1997) *Cell* **88,** 593–602.
41. Nevins, J. R. (2001) *Hum. Mol. Genet.* **10,** 699–703.
42. Herrera, R. E., Sah, V. P., Williams, B. O., Makela, T. P., Weinberg, R. A. & Jacks, T. (1996) *Mol. Cell. Biol.* **16,** 2402–2407.
43. Ali, S. H. & DeCaprio, J. A. (2001) *Semin. Cancer Biol.* **11,** 15–23.
44. Rodriguez-Puebla, M. L., Robles, A. I. & Conti, C. J. (1999) *Mol. Carcinog.* **24,** 1–6.
45. DiGiovanni, J., Bhatt, T. S. & Walker, S. E. (1993) *Carcinogenesis* **14,** 319–321.
46. Robles, A. I., Rodriguez-Puebla, M. L., Glick, A. B., Trempus, C., Hansen, L., Sicinski, P., Tennant, R. W., Weinberg, R. A., Yuspa, S. H. & Conti, C. J. (1998) *Genes Dev.* **12,** 2469–2474.
47. Denissenko, M. F., Pao, A., Tang, M. & Pfeifer, G. P. (1996) *Science* **274,** 430–432.
48. Denissenko, M. F., Venkatachalam, S., Ma, Y. H. & Wani, A. A. (1996) *Mutat. Res.* **363,** 27–42.
49. Kamimura, A., Kamachi, M., Nishihira, J., Ogura, S., Isobe, H., Dosaka-Akita, H., Ogata, A., Shindoh, M., Ohbuchi, T. & Kawakami, Y. (2000) *Cancer* **89,** 334–341.
50. Petrenko, O., Fingerle-Rowson, G., Peng, T., Mitchell, R. A. & Metz, C. N. (2003) *J. Biol. Chem.* **278,** 11078–11085.
51. Yamasaki, L., Bronson, R., Williams, B. O., Dyson, N. J., Harlow, E. & Jacks, T. (1998) *Nat. Genet* **18,** 360–364.
52. Cloud, J. E., Rogers, C., Reza, T. L., Ziebold, U., Stone, J. R., Picard, M. H., Caron, A. M., Bronson, R. T. & Lees, J. A. (2002) *Mol. Cell. Biol.* **22,** 2663–2672.
53. Attardi, L. D., Lowe, S. W., Brugarolas, J. & Jacks, T. (1996) *EMBO J.* **15,** 3693–3701.
54. Zhao, R., Gish, K., Murphy, M., Yin, Y., Notterman, D., Hoffman, W. H., Tom, E., Mack, D. H. & Levine, A. J. (2000) *Genes Dev.* **14,** 981–993.
55. Espinosa, J. M. & Emerson, B. M. (2001) *Mol Cell.* **8,** 57–69.
56. Ard, P. G., Chatterjee, C., Kunjibettu, S., Adside, L. R., Gralinski, L. E. & McMahon, S. B. (2002) *Mol. Cell. Biol.* **22,** 5650–5661.
57. Murphy, M., Ahn, J., Walker, K. K., Hoffman, W. H., Evans, R. M., Levine, A. J. & George, D. L. (1999) *Genes Dev.* **13,** 2490–2501.
58. Marson, A. L., Tarr, D. E. & Scott, A. L. (2001) *Gene* **278,** 53–62.
59. Jaworski, D. C., Jasinskas, A., Metz, C. N., Bucala, R. & Barbour, A. G. (2001) *Insect Mol. Biol.* **10,** 323–331.
60. Swope, M. D. & Lolis, E. (1999) *Rev. Physiol. Biochem. Pharmacol.* **139,** 1–32.
61. Jiang, D., Lenardo, M. J. & Zuniga-Pflucker, C. (1996) *J. Exp. Med.* **183,** 1923–1928.
62. Nacht, M., Strasser, A., Chan, Y. R., Harris, A. W., Schlissel, M., Bronson, R. T. & Jacks, T. (1996) *Genes Dev.* **10,** 2055–2066.
63. Albina, J. E., Cui, S., Mateo, R. B. & Reichner, J. S. (1993) *J. Immunol.* **150,** 5080–5085.
64. Sarih, M., Souvannavong, V. & Adam, A. (1993) *Biochem. Biophys. Res. Commun.* **191,** 503–508.
65. Mitchell, R. A., Laio, H., Chesney, J., Fingerle-Rowson, G., Baugh, J., David, J. & Bucala R. (2002) *Proc. Natl. Acad. Sci. USA* **99,** 345–350.
66. Ekbom, A. (1998) *J. Gastrointest. Surg.* **2,** 312–313.
67. Graham, D. Y. (2000) *J. Gastroenterol.* **35,** 90–97.